

# Carbon Nanohoos: Multiple Molecular Templates for Exploring Spectroscopic, Electronic, and Thermoelectric Properties

Oday A. Al-Owaedi\*

Cite This: *ACS Omega* 2024, 9, 10610–10620

Read Online

ACCESS |



Metrics &amp; More



Article Recommendations



Supporting Information

**ABSTRACT:** A combination of density functional theory (DFT) methods and quantum transport theory (QTT) has been used to investigate the spectroscopic, electronic, and thermoelectric properties of carbon nanohoop molecules with different molecular templates. The connectivity type, along with inherent strain, impacts the transport behavior and creates a destructive quantum interference (DQI), which proves itself to be a powerful strategy to enhance the thermoelectric properties of these molecules, making them promising candidates for thermoelectric applications.



## INTRODUCTION

The individual and unique morphology of carbon-based materials has made them a goal of many studies investigating the chemical and physical properties of devices based on these materials over the past century.<sup>1–5</sup> One of these materials is the carbon nanohoop (CNH), which has attracted wide interest and many applications, such as organic electronics,<sup>6,7</sup> supramolecular sensing,<sup>8–10</sup> and bioimaging.<sup>11</sup> The planarity of sp<sup>2</sup>-carbon centers,<sup>12</sup> which form  $\pi$ -orbitals, has granted the CNH molecules an attractive functionality as incarnated by their unique charge transport properties. In this context, Terri C. Lovell et al.<sup>6</sup> demonstrated that the strain played a central role in defining the properties of carbon nanohoos and controlling the photophysical properties of these molecules, which are particularly exciting. In addition, Ramesh Jasti et al.<sup>1</sup> theoretically investigated the structural and optical properties of the carbon nanohoop molecules, and they proved that the favored geometry for the even-membered nanohoos, [12]- and [18]cycloparaphenylene, was a staggered configuration in which the dihedral angle between two adjacent phenyl rings alternated between 33 and 34°, respectively. Furthermore, the effect of the strain in the  $\pi$ -conjugated hoop molecules<sup>13</sup> on the structural, spectroscopic, and optical properties of cycloparaphenylacetylene (CPP) and cycloparaphenylene molecules has been studied widely via many research studies.<sup>12,14–19</sup> On a few occasions, the charge transport properties of nanohoos were studied. Kayahara et al.<sup>7</sup> reported that CPP molecules might be interesting materials for charge storage due to their rigid structure, intrinsic porosity, and tunable properties. However, in only one case was the application of a CPP derivative investigated for charge storage.<sup>20,21</sup> The bending of aromatic units could lead to the lack of synthetic generality and low stability, but the property of preservation of the radial conjugation of  $\pi$ -orbitals that distinguished these molecules, assisting the formation of CHN structures in different shapes such as circle, square, and triangle templates, as well as rectangle and star structure shapes.<sup>22</sup> Exploring the spectroscopic,

electronic, and thermoelectric properties of CNH molecules with different molecular templates provides more insights into the structure–property relationship and may answer fundamental questions on the topic of quantum interference (QI) in single-molecule junctions.<sup>23–30</sup> A tunneling process pictures the coherent electron transport through a metal–molecule–metal sandwich structure.<sup>31</sup> Quantum interference is not only one of the phenomena that characterizes<sup>32,33</sup> the tunneling transport but also controls most of the properties of molecular junctions.<sup>23–30</sup> Carbon nanohoop molecules and their derivatives could be a perfect candidate to explore quantum interference (QI), since they provide a powerful way to investigate the propagation of de Broglie waves through source |molecule| drain configuration. If the phases of the propagated waves are identical, then constructive quantum interference (CQI) occurs, leading to effective transport and high electrical conductance.<sup>34–38</sup> In contrast, if the waves are out of phase, then destructive quantum interference (DQI) occurs and the transport is blocked.<sup>39–43</sup> The spectroscopic<sup>1,44–46</sup> and optical<sup>47–49</sup> properties of carbon nanohoos have been studied widely, but the investigation of QI effect on electronic and thermoelectric properties of this kind of molecules is limited. Therefore, this work aims to explore the impact of QI on these properties using a combination of density functional theory (DFT) methods<sup>49,50</sup> and quantum transport theory (QTT).<sup>50–61</sup>

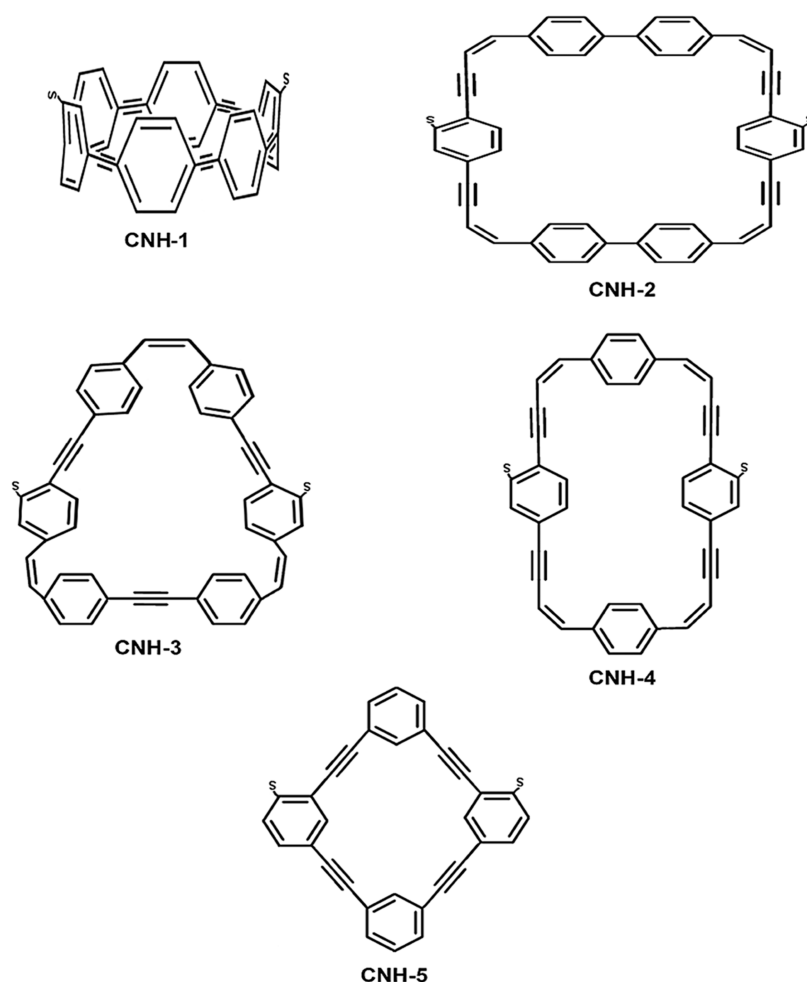
Received: November 9, 2023

Revised: January 30, 2024

Accepted: February 6, 2024

Published: February 22, 2024





**Figure 1.** Schematic illustration of carbon nano hoop molecules in different molecular templates.

## THEORETICAL METHODS


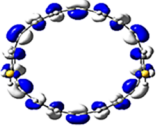

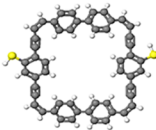
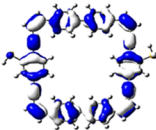
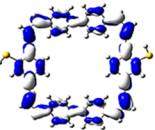
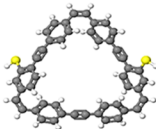
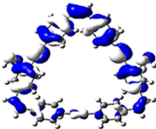
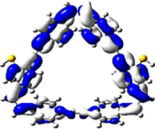
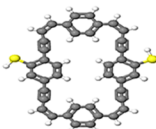
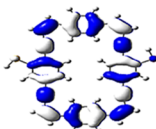
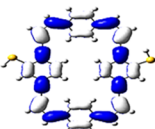
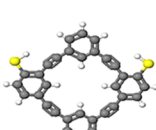
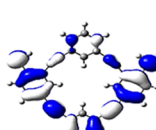
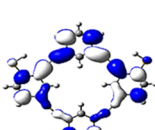
The initial optimization of gas-phase molecules, isosurfaces, and spectroscopic calculations was carried out at the B3LYP level of theory<sup>62</sup> with the 6-31G\*\* basis set<sup>63,64</sup> using density functional theory (DFT) and time-dependent DFT (TD-DFT).<sup>65</sup> The geometric optimization of all gold |molecule| gold configurations under investigation in this work was carried out by the implementation of DFT<sup>50,51</sup> in the SIESTA<sup>50</sup> code, as shown in Figure S2 (see the Supporting Information). The generalized gradient approximation (GGA) of the exchange–correlation functional was used with a double- $\zeta$  polarized (DZP) basis set, a real-space grid defined with an equivalent energy cutoff of 250 Ry. The geometry optimization for each structure is performed to force smaller than 20 meV/Å. The mean-field Hamiltonian obtained from the converged DFT calculations was combined with the GOLLUM<sup>53</sup> code. The quantum transport theory (QTT)<sup>52–61</sup> implemented in GOLLUM has been used to calculate the electronic and thermoelectric properties of all molecular junctions.

## RESULTS AND DISCUSSION

A family of five carbon nano hoop molecules was chosen for the study here, as shown in Figure 1. In the quest to investigate the effect of the strain and connectivity type on the properties of molecules, the molecules under investigation were selected with five different shapes.

Figure 1 shows that the first molecule (CNH-1) has a circular shape, while the second molecule (CNH-2) has a square structure. The third molecule (CNH-3) possesses a structure shape close to triangular. A rectangular shape is the closest picture of the fourth molecule (CNH-4), and the matching description of molecule five (CNH-5) is the star-shaped structure. These molecules are cycloparaphenylene (CPP) molecules, which are typical  $\pi$ -conjugated molecules consisting solely of phenyl rings connected at the para-position, except for the molecule (CNH-5) in which phenyl rings are connected at ortho and meta positions. Shigeru et al.<sup>12</sup> mentioned that the strain impact is a crucial parameter in this kind of molecule. Therefore, this work seeks to explore the molecular shape effect on the strain and thus the properties of these molecules. The choice of molecule CNH-5 with a star-shaped structure is to obtain more insights into the role of different connectivities (para or meta) between phenyl rings in creating constructive or destructive interference.

The orbital distribution and the electronic structure of molecules were investigated, and the plots of the optimized structures and the highest occupied and lowest unoccupied molecular orbitals (HOMO and LUMO, respectively) are given in Figure 2. The HOMOs of all molecules display a familiar pattern of  $\pi$ – $\pi$  interactions along the molecular backbone. The LUMOs are also localized over the molecular backbones and could be described as a  $\pi$ -conjugated system. In addition, Figure 2 and Table 1 show that the values of the HOMO–LUMO gap

Molecule	Structure	HOMO (eV)	LUMO (eV)	$a_H \cdot a_L$
CNH-1		 -5.17	 -2.53	- CQI
CNH-2		 -5.36	 -2.51	- CQI
CNH-3		 -5.38	 -1.99	- CQI
CNH-4		 -5.31	 -2.72	- CQI
CNH-5		 -5.83	 -1.97	+ CQI

**Figure 2.** Optimized geometry of all molecules in a gas phase (structure), HOMOs, and LUMOs (isosurfaces  $\pm 0.02$  ( $e/\text{bohr}^3$ )<sup>1/2</sup>). The white part has a positive sign, and the blue part has a negative sign.  $a_H \cdot a_L$  is the multiplication of the HOMO and LUMO amplitudes. As an example, when HOMO and LUMO for the CNH-1 molecule possess different signs, then the multiplication of molecular orbital amplitudes ( $a_H \cdot a_L$ ) has a negative sign, and the molecule exhibits CQI.

**Table 1.**  $H-L$  Gap is the HOMO–LUMO Gap,  $A$  is the Absorption Intensity,  $\lambda_{\text{max}}^A$  is the Maximum Absorption Wavelength,  $E$  is the Emission Intensity,  $\lambda_{\text{max}}^E$  is the Maximum Emission Wavelength,  $f_{\text{em}}$  is Emission Oscillator Strength, and SS is the Stokes Shift

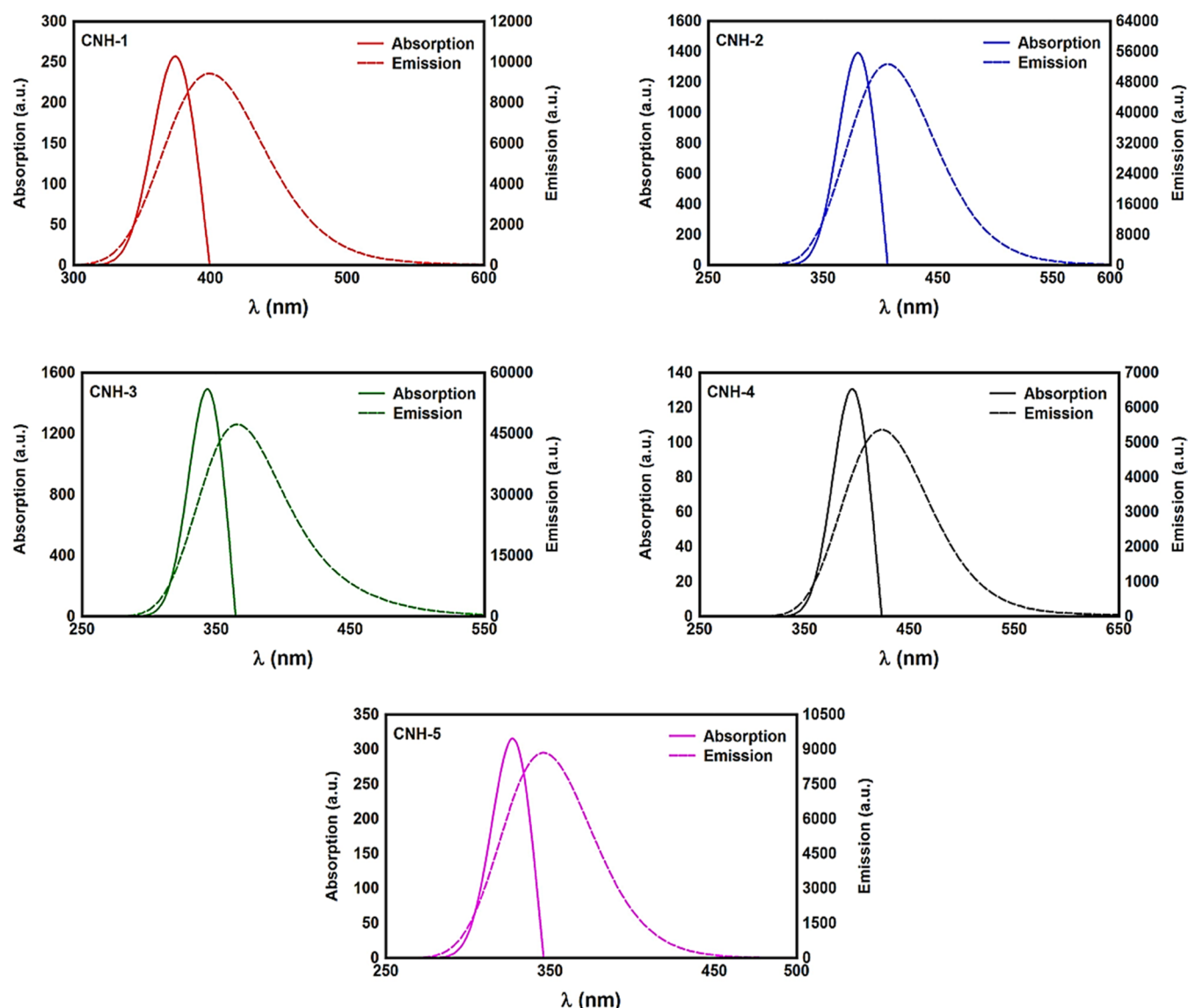
molecule	$H-L$ gap (eV)	$A$ (a.u.)	$\lambda_{\text{max}}^A$ (nm)	$E$ (a.u.)	$\lambda_{\text{max}}^E$ (nm)	$f_{\text{em}}$	SS (nm)
CNH-1	2.64	257.1	374.4	9433.6	399.6	0.13	25.2
CNH-2	2.85	1392.5	379.8	52723.4	406.8	1.3	27
CNH-3	3.39	1492.6	343.6	47238.5	365.2	1.13	21.6
CNH-4	2.59	130.7	396	5355.3	424.8	0.11	28.8
CNH-5	3.86	315.4	326.8	8846.8	345.7	0.22	18.9

have fluctuated, and the highest value (3.86 eV) was given by molecule CNH-5, while the lowest value (2.59 eV) was exhibited by molecule CNH-4. These results are consistent with previous studies.<sup>12</sup> They reported that the HOMO and LUMO of cycloparaphenylenes (CPPs) rings become higher and lower in energy, respectively, as the number of paraphenylene units decreases due to the decrease of the effective  $\pi$ -conjugation. Furthermore, the calculated values of the HOMO–LUMO gap ranged from 2.59 to 3.86 eV, which are close to the HOMO–LUMO gap of the  $C_{60}$  molecule, indicating that the carbon nano hoop is a promising molecule for material applications.<sup>66</sup>

In order to explore the impact of connectivity type and to prove the existence of CQI and DQI in carbon nano hoop molecules, the current investigation performed an orbital analysis and demonstrated that CQI was dominated on the transport of all molecular junctions, except the transport through the CNH-5 molecular junction, which is dominated by DQI, as shown in Figure 2. Lambert et al.<sup>67</sup> reported an orbital symmetry rule. The magic ratio theory<sup>68</sup> is based on utilizing the exact core Green's function defined as follows.

$$g(E) = (IE - H)^{-1} \quad (1)$$

In the literature, various approximations to  $g(E)$  are discussed, one of which involves the approximation of including only the



**Figure 3.** UV/vis absorption spectra (solid curves) and emission spectra (dashed curves) for all molecules.

contributions to  $g(E)$  from the HOMO and LUMO. If the amplitudes of the HOMO on sites  $a$  and  $b$  are denoted  $\psi_a^{E_H}$  and  $\psi_b^{E_H}$  and the amplitudes of the LUMO are  $\psi_a^{E_L}$  and  $\psi_b^{E_L}$ , respectively, and the contributions from all other orbitals are ignored, then a crude approximation to Green's function  $g_{ba}(E)$  is

$$g_{ab}(E) \approx \frac{\psi_a^{(E_H)}\psi_b^{(E_H)}}{E - E_H} + \frac{\psi_a^{(E_L)}\psi_b^{(E_L)}}{E - E_L} \quad (2)$$

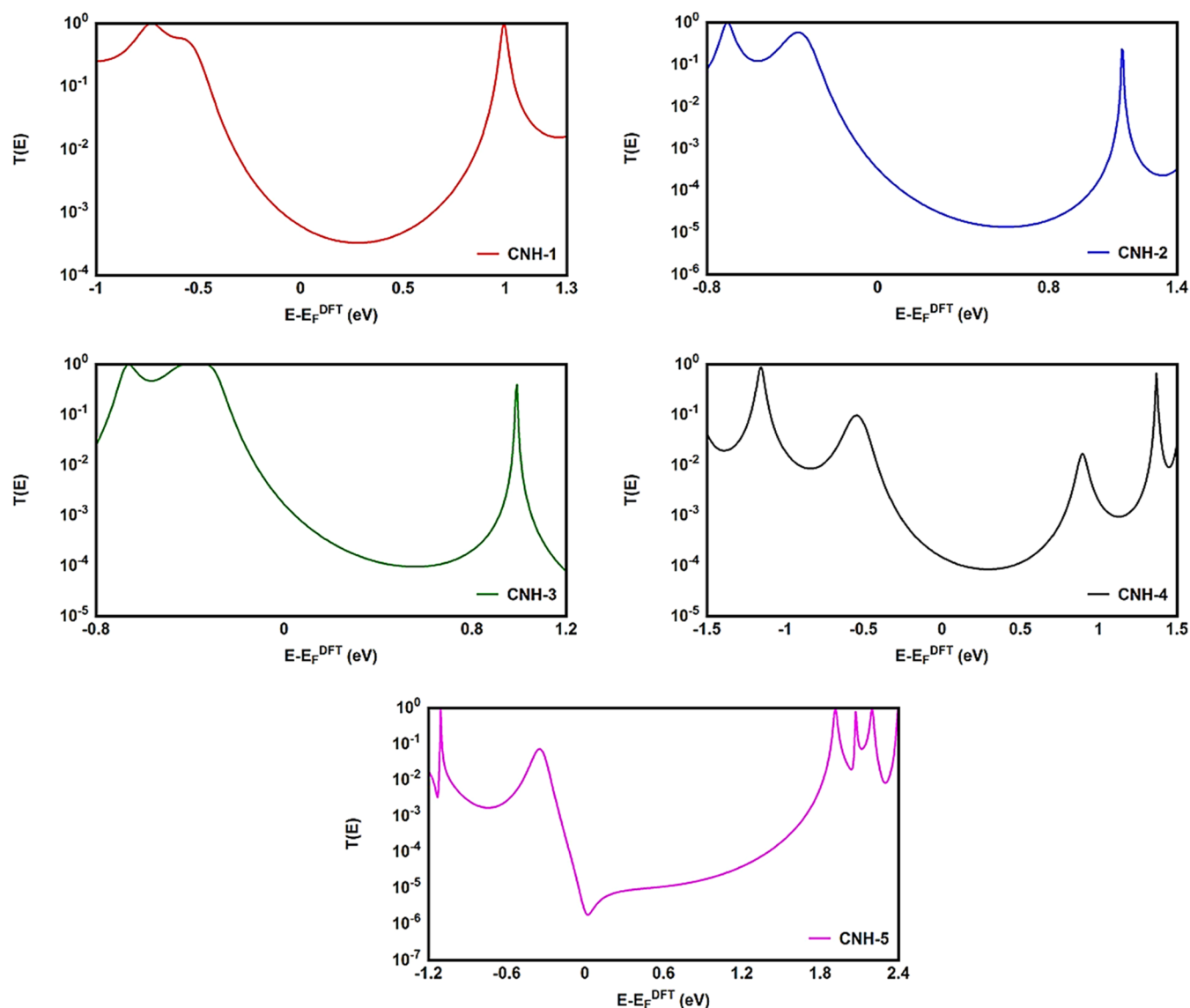
where  $E_H$  and  $E_L$  are the energies of the HOMO and LUMO, respectively. If the HOMO product  $\psi_b^{E_H}\psi_a^{(E_H)}$  has the same sign as the LUMO product  $\psi_b^{(E_L)}\psi_a^{(E_L)}$ , then the right-hand side of eq 2 will vanish for some energy  $E$  in the range  $E_H \leq E \leq E_L$ . In this case, one can say that the HOMO and LUMO interfere destructively. On the other hand, if the HOMO and LUMO products have opposite signs, then the right-hand side of eq 2 will not vanish within the HOMO–LUMO gap and one can say that the HOMO and LUMO interfere constructively within the gap. (They could of course interfere destructively for some other energy  $E$  outside the gap.) When the right-hand side of eq 2 vanishes, the main contribution to  $g_{ba}(E)$  comes from all other

orbitals, so in general, eq 2 could be a poor approximation. One exception to this occurs when the lattice is bipartite because the Coulson–Rushbrooke (CR) theorem<sup>69</sup> tells us that if  $a$  and  $b$  are both even or both odd, then the orbital products on opposite sides of eqs 3 and 4 have the same sign. Consequently, when the HOMO and LUMO interfere destructively, all other pairs of orbitals interfere destructively, leading to the trivial zeros in the magic number table,<sup>68</sup> for which  $g_{ba}(0) = 0$ .

$$\psi_a^{(E_n)}\psi_b^{(E_n)} = \psi_a^{(-E_n)}\psi_b^{(-E_n)} \quad (3)$$

$$\phi_b^{(E_n)}\phi_b^{(E_n)} = \phi_b^{(-E_n)}\phi_b^{(-E_n)} \quad (4)$$

Here,  $\pm E_n$  are eigenvalues in  $\pm$  pairs, and the eigenstate belonging to  $-E_n$  is related to the eigenstate belonging to  $E_n$ . Obviously, this exact cancellation is a property of bipartite lattices only, but based on its success for bipartite lattices, one might suppose that eq 2 is a reasonable approximation for other lattices. Nevertheless, as pointed out by Yoshizawa et al.,<sup>70–73</sup> since orbitals such as those in Figure 2 are often available from DFT calculations, it can be helpful to examine the question of



**Figure 4.** Transmission coefficient  $T(E)$  as a function of the electron energies for all molecules.

whether or not the HOMO and LUMO (or indeed any other pair of orbitals) interfere destructively or constructively, by examining the colors of orbitals. This is simplified by writing eq 2 in the following form

$$g_{ab}(E) \approx \frac{a_H}{E - E_H} + \frac{a_L}{E - E_L} \quad (5)$$

where  $a_H = \psi_a^{(E_H)} \psi_b^{(E_H)}$  and  $a_L = \psi_a^{(E_L)} \psi_b^{(E_L)}$ . If the HOMO product  $a_H$  has the same sign as the LUMO product  $a_L$ , then the right-hand side of eq 5 will vanish for some energy  $E$  in the range  $E_H \leq E \leq E_L$ . In other words, HOMO and LUMO will interfere destructively for some energy within the HOMO–LUMO gap. However, this does not mean that the exact  $g_{ba}(E)$  will vanish. Indeed, if the right-hand side of eq 5 vanishes, then the contributions from all other orbitals become the dominant terms.<sup>74</sup> Nevertheless, this is an appealing method of identifying QI effects in molecules and describing their qualitative features.<sup>75</sup>

The distinctive properties of carbon nano hoops including for example their spectroscopic properties, especially the absorption and emission spectra, have become the subject of the increased

interest for many scientific studies.<sup>76</sup> Interestingly, the UV/visible absorption and emission spectra showed asymmetric peaks, since the range of the absorption spectra extends from 326.8 to 396 nm, as shown in Table 1, and the emission spectra ranges from 345.7 to 424.8 nm. These results could be interpreted in terms of strain and molecular shape effects, which are critical qualities that endow molecules with atypical spectroscopic properties and reactivity, since the inherent strain of the molecule increases with the decrease of the carbon nano hoop size and consequently changes the structural and spectroscopic properties. In fact, the carbon nano hoops (CNH-5 and CNH-4) possess the poorest geometry for the orbital overlap and the fewest number of aryl rings. Thus, these molecules are expected to have a small size, which in turn leads to a smaller optical absorption gap<sup>47</sup> than that of large-size molecules (CNH-1, CNH-2, and CNH-3). These results are consistent with the results of refs 1,12,77. Furthermore, Figure 3 and Table 1 show that the Stokes shift of these molecules is lowered with a decrease of size, and the values of Stokes shift range from 18.9 to 27 nm. These results may introduce CNH-4

and CNH-2 molecules as promising candidates for encryption and medical applications.<sup>78,79</sup>

One of the most important parameters in optoelectronic applications is the emission oscillator strength ( $f_{em}$ ).<sup>80</sup> Theoretically, for a given PL material,  $f_{em}$  is directly proportional to the emission cross section ( $\sigma_{em}$ ), which is given by<sup>81</sup>

$$\sigma_{em}(\nu) = \frac{e^2}{4\epsilon_0 m_e c_0 n_F} g(\nu) f_{em} \quad (6)$$

where  $e$  is the electron charge,  $\epsilon_0$  is the vacuum permittivity,  $m_e$  is the mass of the electron,  $c_0$  is the speed of light,  $n_F$  is the refractive index of the gain material,  $\nu$  is the frequency of the corresponding emission, and  $g(\nu)$  is the normalized line shape function with  $\int g(\nu) d\nu = 1$ . Table 1 shows that two molecules (CNH-2 and CNH-3) have  $f_{em}$  values of 1.3 and 1.13, respectively. These results could be ascribed to the highest intensity value of the emission spectra of these molecules (52723.4 and 47238.5 au, respectively), indicating the highest HOMO  $\rightarrow$  LUMO transition rate in these molecules, which might be attributed to an increase in their emission cross section ( $\sigma_{em}$ ), suggesting that CNH-2 and NH3 are appropriate molecules for optoelectronic applications.

In this work,  $T(E)$  has been calculated by attaching the optimized molecules with two (111)-directed gold electrodes, which involve two small layers (each one consists of 6-atoms pyramidal gold lead), and seven layers of (111)-oriented bulk gold with each layer consisting of  $6 \times 6$  atoms, and a layer spacing of 0.235 nm to create molecular junctions, (see the Supporting Information for all models). These layers were then further repeated to yield infinitely long gold electrodes, which carry the electric current. From these molecular junctions, electronic and thermoelectric properties were calculated using the GOLLUM code.<sup>53</sup> The transmission coefficient according to the Landauer–Büttiker<sup>82</sup> formalism is given by

$$T(E) = T_r \{ \Gamma_R(E) G^R(E) \Gamma_L(E) G^{R\dagger}(E) \} \quad (7)$$

where

$$\Gamma_{L,R}(E) = i \left( \sum_{L,R} (E) - \sum_{L,R}^{\dagger} (E) \right) \quad (8)$$

where  $\Gamma_{L,R}$  describes the level broadening due to the coupling between left ( $L$ ) and right ( $R$ ) electrodes and the central scattering region, and  $\sum_{L,R}(E)$  are the retarded self-energies associated with this coupling.

$$G^R = (EX - H - \Sigma_L - \Sigma_R)^{-1} \quad (9)$$

Here,  $G^R$  is the retarded Green's function,  $H$  is the Hamiltonian, and  $X$  is the overlap matrix. The transport properties are then calculated using the following Landauer formula

$$(E_F T) = G_O \int_{-\infty}^{\infty} \det(E) [-\partial f(E, T, E_F) / \partial E] \quad (10)$$

where  $f$  is the Fermi–Dirac probability distribution function.

Figure 4 shows the transmission coefficient  $T(E)$ <sup>83</sup> of source | molecule | drain molecular junctions. The signature of constructive quantum interference (CQI) is clear for the first four molecules, which leads to high  $T(E)$  values, as shown in Figure 4 and Table 2. These outcomes are ascribed to the para connectivity<sup>84–89</sup> between phenyl rings. In contrast, an antiresonance feature appears at the middle of the HOMO–LUMO gap in the transport curve of the CNH-5 molecule,

**Table 2. Transmission Coefficient  $T(E)$ , Molecule Length ( $l = S \cdots S$ ), Highest Occupied Molecular Orbitals of the Molecules in a Junction ( $J^{HOMO}$ ), Lowest Unoccupied Molecular Orbitals of the Molecules in a Junction ( $J^{LUMO}$ ), and HOMO–LUMO Gap ( $J^{H-L}$  Gap) of the Molecules in a Junction**

molecule	$T(E)$	$l$ (nm)	$J^{HOMO}$ (eV)	$J^{LUMO}$ (eV)	$J^{H-L}$ gap (eV)
CNH-1	$5.99 \times 10^{-4}$	1.361	0.27	0.86	1.13
CNH-2	$3.14 \times 10^{-4}$	1.723	0.25	1.13	1.38
CNH-3	$1.63 \times 10^{-3}$	1.083	0.31	0.98	1.29
CNH-4	$1.51 \times 10^{-4}$	1.292	0.31	0.95	1.26
CNH-5	$2.06 \times 10^{-6}$	1.295	0.34	0.88	1.22

which is a representation of the destructive quantum interference (DQI).<sup>25–27,32,33,39</sup> Herein, the meta connectivity between phenyl rings results in the lowest  $T(E)$  value. In addition, the values of  $T(E)$  for CHN-1, CNH-2, and CNH-4 molecules are close to each other and smaller than that of the CNH-3 molecule, as shown in Table 2. These results could be understood in terms of the inherent strain, which resulted in the molecular shape effect ( $\approx$  a triangular shape) and in turn decreased the tunneling distance ( $l$ ) for the CNH-3 molecule and consequently increased  $T(E)$ , according to eq 11.

$$T(E) \propto e^{-\beta l} \quad (11)$$

Here,  $T(E)$  is the transmission coefficient,  $\beta$  is the electronic decay constant, and  $l$  is the tunneling distance. In addition, the molecule length of compounds studied here of ca.  $> 2$  nm is consistent with a dominant contribution from the coherent tunneling mechanism.<sup>90–93</sup> The rectangular tunnel barrier model<sup>94</sup> states that the electrical conductance through a single molecule (barrier) decreases exponentially with the length of the barrier, according to eq 11.

With the integration of these results with spectroscopic results, there is a prediction that the first four molecules might be promising candidates for electronic and optoelectronic applications.

Exploring the influence of DQI on the transport behavior and consequently on the thermoelectric properties is one of the main goals of this work. The slope of  $T(E)$  determines the Seebeck coefficient ( $S$ ) and thus the electronic figure of merit ( $Z_{el}T$ ). The Seebeck coefficient ( $S$ ), power factor ( $P$ ), and ( $Z_{el}T$ ) are given by

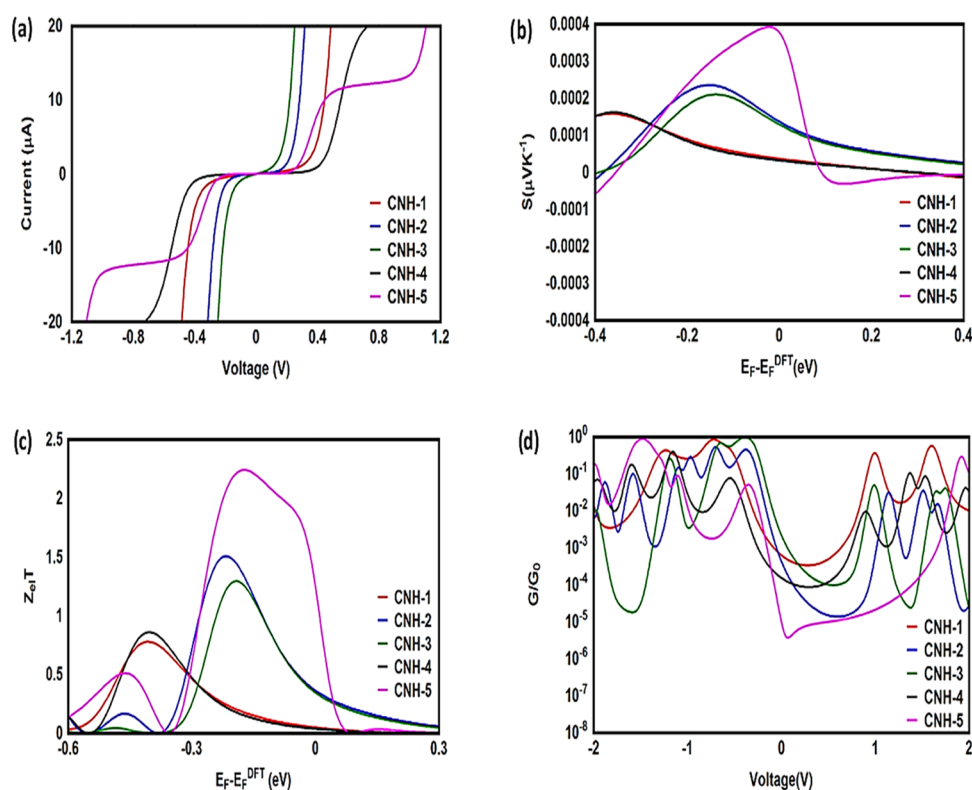
$$S \approx -L|e|T \left( \frac{d \ln T(E)}{dE} \right)_{E=E_F} \quad (12)$$

where  $L$  is the Lorenz number  $L = \left( \frac{k_B}{e} \right)^2 \frac{\pi^2}{3} = 2.44 \times 10^{-8} \text{ W}\Omega\text{K}^{-2}$ . In other words,  $S$  is proportional to the negative slope of  $\ln T(E)$ , evaluated at the Fermi energy. Based on the Seebeck coefficient, the power factor was calculated by

$$P = GS^2T \quad (13)$$

where  $T$  is the temperature  $T = 300$  K,  $G$  is the electrical conductance, and  $S$  is the Seebeck coefficient, and the purely electronic figure of merit ( $Z_{el}T$ ) is given by<sup>95,96</sup>

$$Z_{el}T = \frac{S^2G}{k_{el}}T = \frac{S^2}{L} \quad (14)$$



**Figure 5.** (a) Current–voltage characteristics, (b) Seebeck coefficient ( $S$ ), (c) electronic figure of merit ( $Z_{ei}T$ ), and (d) electrical conductance ( $G/G_0$ ) as a function of the voltage of all molecular junctions.

where  $k_{el}$  is the electron thermal conductance. According to previous studies,<sup>95,96</sup> the figure of merit in this work has been calculated only based on a purely electronic contribution.

It is well known that the performance of thermoelectric materials is characterized by an efficient conversion of input heat to electricity.<sup>97,98</sup> In this context, the enhancement of power factor ( $P$ ) and electronic figure of merit ( $Z_{ei}T$ ), which depend on the Seebeck coefficient ( $S$ ), is important. Figure 5bc and Table 3

**Table 3. Electrical Conductance ( $G$ ), Seebeck Coefficient ( $S$ ), Power Factor ( $P$ ), Electronic Figure of Merit ( $Z_{ei}T$ ), and Threshold Voltage ( $V_{th}$ ) of all Molecular Junctions**

molecule	$G/G_0$	$S$ ( $\mu\text{VK}^{-1}$ )	$P$ ( $\text{WK}^{-1}$ ) $\times 10^{-17}$	$Z_{ei}T$	$V_{th}$ (V)
CNH-1	$0.46 \times 10^{-7}$	3.62	6.11	0.048	0.36
CNH-2	$0.24 \times 10^{-7}$	13.45	44.14	0.35	0.21
CNH-3	$0.12 \times 10^{-6}$	12.67	204.06	0.33	0.15
CNH-4	$0.11 \times 10^{-7}$	3.13	1.11	0.036	0.44
CNH-5	$0.16 \times 10^{-9}$	37.24	2.22	1.17	0.29

show that the highest values of  $S$  and  $Z_{ei}T$  ( $37.24 \mu\text{VK}^{-1}$  and 1.17, respectively) have been exhibited by molecule CNH-5. In contrast, molecule CNH-4 presented the lowest values of these parameters ( $3.13 \mu\text{VK}^{-1}$  and 0.036, respectively). These results not only demonstrated the important role of DQI in the improvement of  $S$  and  $Z_{ei}T$  for molecule CNH-5 but also established a crucial role of the inherent strain in the CNH-4 molecule, which might contribute to lowering the values of  $S$  and  $Z_{ei}T$ . In addition, the competition between electrical conductance and the Seebeck coefficient according to eq 13 led to the power factor order of  $P_{\text{CNH-3}} > P_{\text{CNH-2}} > P_{\text{CNH-1}} > P_{\text{CNH-5}} > P_{\text{CNH-4}}$ . In light of the aforementioned results, these molecules

could be considered promising candidates for thermoelectric applications. Furthermore, Figure 5a and Table 3 present the current–voltage ( $I$ – $V$ ) characteristics of all molecular junctions, which are limited to the first and third quadrants of the  $I$ – $V$  plane crossing the origin. Therefore, they are classified as components that consume electric power, and here, the importance of the threshold voltage ( $V_{th}$ ) value appears.

The values of  $V_{th}$  range from 0.15 to 0.44 V, which makes these molecules promising candidates for electronic applications. Moreover,  $I$ – $V$  characteristics of all molecular junctions exhibited a semiconductor behavior, except for the CNH-5 molecule, which shows the quantum staircase structure in the conductance. Obviously, as the voltage increases, the density of electrons also increases, which leads to an increase in the number of occupied subbands. The dependence conductance, in this case, is a set of plateaus separated by steps of height  $2e^2/h$ : a stepwise change in the conductance of the CNH-5 molecule channels occurs each time the Fermi level coincides with one of the subbands. Hence, the quantum staircase behavior could be attributed to the adiabatic transparency of spin-nondegenerate subbands of the CNH-5 molecule.<sup>75,99</sup>

## CONCLUSIONS

In conclusion, the type of connectivity whether it is meta or para along with the molecular shape effect is a crucial parameter in controlling and improving the spectroscopic, electronic, and thermoelectric properties of carbon nanohoop molecules. In addition, this work has concluded that the inherent strain plays an important role in governing transport behavior. The most important conclusion is that carbon nanohoop molecules are a perfect host to examine the destructive quantum interference, which proved itself to be a robust strategy to enhance the

thermoelectric properties of these molecules, making them a suitable material for thermoelectric applications. The spectroscopic results provided a considerable body of information for designing effective materials for optoelectronic, encryption, and medical applications.

## ■ ASSOCIATED CONTENT

### SI Supporting Information

The Supporting Information is available free of charge at <https://pubs.acs.org/doi/10.1021/acsomega.3c08944>.

Theories and all details relevant to the computational methods, as well as the theoretical models of all source | molecule drain configurations<sup>100–115</sup> (PDF)

## ■ AUTHOR INFORMATION

### Corresponding Author

Oday A. Al-Owaedi – Department of Laser Physics, College of Science for Women, University of Babylon, Babylon 51001 Hilla, Iraq; Al-Zahrawi University College, Holy Karbala, Najaf 56001, Iraq; [orcid.org/0000-0003-0721-0409](https://orcid.org/0000-0003-0721-0409); Email: [oday.alowaedi@uobabylon.edu.iq](mailto:oday.alowaedi@uobabylon.edu.iq)

Complete contact information is available at: <https://pubs.acs.org/10.1021/acsomega.3c08944>

### Notes

The author declares no competing financial interest.

## ■ ACKNOWLEDGMENTS

O.A.A. thanks the University of Babylon and Al-Zahrawi University College for their support.

## ■ REFERENCES

- Jasti, R.; Bhattacharjee, J.; Neaton, J. B.; Bertozzi, C. R. Synthesis, Characterization, and Theory of [9]-, [12]-, and [18]-Cycloparaphenylene: Carbon Nanohoop Structures. *J. Am. Chem. Soc.* **2008**, *130*, 17646–17647.
- Yamago, S.; Watanabe, Y.; Iwamoto, T. Synthesis of [8] Cycloparaphenylene from a Square-Shaped Tetranuclear Platinum Complex. *J. Angew. Chem. Int. Ed.* **2010**, *49*, 757–759.
- Omachi, H.; Matsuura, S.; Segawa, Y.; Itami, K. A Modular and Size-Selective Synthesis of [n] Cycloparaphenylenes: A Step toward the Selective Synthesis of [n,n] Single-Walled Carbon Nanotubes. *J. Angew. Chem. Int. Ed.* **2010**, *49*, 10202–10205.
- Patel, V. K.; Kayahara, E.; Yamago, S. Practical Synthesis of [n] Cycloparaphenylenes (n = 5,7–12) by H<sub>2</sub>SnCl<sub>4</sub>-Mediated Aromatization of 1,4-Dihydroxycyclo-2,5-diene Precursors. *Chem. - Eur. J.* **2015**, *21*, 5742–5749.
- Darzi, E. R.; White, B. M.; Loventhal, L. K.; Zakharov, L. N.; Jasti, R. An Operationally Simple and Mild Oxidative Homocoupling of Aryl Boronic Esters to Access Conformationally Constrained Macrocycles. *J. Am. Chem. Soc.* **2017**, *139*, 3106–3114.
- Terri, C. L.; Curtis, E. C.; Lev, N. Z.; Ramesh, J. Symmetry Breaking and the Turn-On Fluorescence of Small, Highly Strained Carbon Nanohoos. *Chem. Sci.* **2019**, *10*, 3786–3790.
- Kayahara, E.; Sun, L.; Onishi, H.; Suzuki, K.; Fukushima, T.; Sawada, A.; Kaji, H.; Yamago, S. Gram-Scale Syntheses and Conductivities of [10] Cycloparaphenylene and Its Tetraalkoxy Derivatives. *J. Am. Chem. Soc.* **2017**, *139*, 18480–18483.
- Iwamoto, T.; Watanabe, Y.; Sadahiro, T.; Haino, T.; Yamago, S. Size-Selective Encapsulation of C<sub>60</sub> by [10] Cycloparaphenylene: Formation of the Shortest Fullerene-Peapod. *J. Angew. Chem. Int. Ed.* **2011**, *50*, 8342–8344.
- Li, P.; Sisto, T. J.; Darzi, E. R.; Jasti, R. The Effects of Cyclic Conjugation and Bending on the Optoelectronic Properties of Paraphenylenes. *Org. Lett.* **2014**, *16*, 182–185.
- Della Sala, P.; Talotta, C.; Caruso, T.; De Rosa, M.; Soriente, A.; Neri, P.; Gaeta, C. Tuning Cycloparaphenylene Host Properties by Chemical Modification. *J. Org. Chem.* **2017**, *82*, 9885–9889.
- White, B. M.; Zhao, Y.; Kawashima, T. E.; Branchaud, B. P.; Pluth, M. D.; Jasti, R. Expanding the Chemical Space of Biocompatible Fluorophores: Nanohoos in Cells. *ACS Cent. Sci.* **2018**, *4*, 1173–1178.
- Shigeru, Y.; Eiichi, K. Synthesis and Reactions of Carbon Nanohoop. *J. Synth. Org. Chem. Jpn.* **2019**, *77*, 1147–1158.
- Ko, U.; Yann, F.; Zhiwei, L.; Kosuke, K.; Masatoshi, K.; Estelle, M.; Ryan, D.; Vojislava, P.; Aya, T.; Ivan, H. Accessing Improbable Foldamer Shapes with Strained Macrocycles. *Chem. - Eur. J.* **2021**, *27*, 11205–11215.
- Yagi, A.; Segawa, Y.; Itami, K. Synthesis and Properties of [9]Cyclo-1,4-naphthylene: A  $\pi$ -Extended Carbon Nanoring. *J. Am. Chem. Soc.* **2012**, *134* (6), 2962–2965.
- Ball, M.; Fowler, B.; Li, P.; Joyce, L. A.; Li, F.; Liu, T.; Paley, D.; Zhong, Y.; Li, H.; Xiao, S.; Ng, F.; Steigerwald, M. L.; Nuckolls, C. Macrocyclization in the Design of Organic n-Type Electronic Materials. *J. Am. Chem. Soc.* **2016**, *138* (39), 12861–12867.
- Ball, M.; Zhong, Y.; Fowler, B.; Zhang, B.; Li, P.; Etkin, G.; Paley, D. W.; Decatur, J.; Dalsania, A. K.; Li, H.; Xiao, S.; Ng, F.; Steigerwald, M. L.; Nuckolls, C. Macrocyclization in the Design of Organic n-Type Electronic Materials. *J. Am. Chem. Soc.* **2016**, *138*, 12861–12867.
- Shuhai, Q.; Yongye, Z.; Li, Z.; Yong, N.; Yanan, W.; Huan, C.; Da-Hui, Q.; Wei, J.; Jishan, W.; He, T.; Zhaohui, W. Axially N-Embedded Quasi-Carbon Nanohoos with Multioxidation States. *CCS Chem.* **2023**, *5*, 1763–1772.
- Ko, U.; Yann, F.; Zhiwei, L.; Kosuke, K.; Masatoshi, K.; Estelle, M.; Ryan, D.; Vojislava, P.; Aya, T.; Ivan, H. Accessing Improbable Foldamer Shapes with Strained Macrocycles. *Chem. - Eur. J.* **2021**, *27*, 11205–11215.
- Xin, Z.; Hyejin, K.; Richard, R. T.; Robert, J. H.; Frank, R. F.; Carson, J. B.; Semin, L. Scalable Synthesis of a [8]-Cycloparaphenyleneacetylene Carbon Nanohoop Using Alkyne Metathesis. *Chem. Commun.* **2021**, *57*, 10887–10890.
- Lucas, F.; Sicard, L.; Jeannin, O.; Rault-Berthelot, J.; Jacques, E.; Quinton, C.; Poriel, C. [4]Cyclo-N-ethyl-2,7-carbazole: Synthesis, Structural, Electronic and Charge Transport Properties. *Chem. - Eur. J.* **2019**, *25*, 7740–7748.
- Furuichi, T.; Inoue, T.; Miyaji, K.; Kanai, K. Anomalous Interfacial Electronic Structure of Solid Films of Non-Planar  $\pi$ -Conjugated Molecule 6-Cycloparaphenylene. *Adv. Mater. Interfaces* **2022**, *9*, No. 2200242.
- Jasti, R.; Bhattacharjee, J.; Neaton, J. B.; Bertozzi, C. R. Synthesis, Characterization, and Theory of [9]-, [12]-, and [18]-Cycloparaphenylene: Carbon Nanohoop Structures. *J. Am. Chem. Soc.* **2008**, *130*, 17646–17647.
- Mayor, M.; Weber, H. B.; Reichert, J.; Elbing, M.; von Hänisch, C.; Beckmann, D.; Fischer, M. Electric Current through a Molecular Rod-Relevance of the Position of the Anchor Groups. *Angew. Chem., Int. Ed.* **2003**, *42*, 5834–5838.
- Taniguchi, M.; Tsutsui, M.; Mogi, R.; Sugawara, T.; Tsuji, Y.; Yoshizawa, K.; Kawai, T. Dependence of Single-Molecule Conductance on Molecule Junction Symmetry. *J. Am. Chem. Soc.* **2011**, *133*, 11426–11429.
- Guédon, C. M.; Valkenier, H.; Markussen, T.; Thygesen, K. S.; Hummelen, J. C.; van der Molen, S. J. Observation of Quantum Interference in Molecular Charge Transport. *Nat. Nanotechnol.* **2012**, *7*, 305.
- Aradhya, S. V.; Meisner, J. S.; Krikorian, M.; Ahn, S.; Parameswaran, R.; Steigerwald, M. L.; Nuckolls, C.; Venkataraman, L. Dissecting Contact Mechanics from Quantum Interference in Single-Molecule Junctions of Stilbene Derivatives. *Nano Lett.* **2012**, *12*, 1643–1647.
- Arroyo, C. R.; Tarkuc, S.; Frisenda, R.; Seldenthuis, J. S.; Woerde, C. H. M.; Elkema, R.; Grozema, F. C.; van der Zant, H. S. J. Signatures



of Quantum Interference Effects on Charge Transport through a Single Benzene Ring. *J. Angew. Chem. Int. Ed.* **2013**, *52*, 3152–3155.

(28) Zhang, Y.; Ye, G.; Soni, S.; Qiu, X.; Krijger, Theodorus, L.; Jonkman, H. T.; Carloti, M.; Sauter, E.; Zharnikov, M.; Chiechi, R. C. Controlling Destructive Quantum Interference in Tunneling Junctions Comprising Self-Assembled Monolayers Via Bond Topology and Functional Groups. *Chem. Sci.* **2018**, *9*, 4414–4423.

(29) Rabache, V.; Chaste, J.; Petit, P.; Della Rocca, M. L.; Martin, P.; Lacroix, J.-C.; McCreery, R. L.; Lafarge, P. Direct Observation of Large Quantum Interference Effect in Anthraquinone Solid-State Junctions. *J. Am. Chem. Soc.* **2013**, *135*, 10218–10221.

(30) Frisenda, R.; Janssen, V. A. E. C.; Grozema, F. C.; van der Zant, H. S. J.; Renaud, N. Mechanically Controlled Quantum Interference in Individual  $\pi$ -Stacked Dimers. *Nat. Chem.* **2016**, *8*, 1099.

(31) Su, T. A.; Neupane, M.; Steigerwald, M. L.; Venkataraman, L.; Nuckolls, C. Chemical Principles of Single-Molecule Electronics. *Nat. Rev. Mater.* **2016**, *1*, No. 16002.

(32) Baghernejad, M.; Yang, Y.; Al-Owaedi, O. A.; Aeschi, Y.; Zeng, B.; Dawood, Z. M.; Li, X.; Liu, J.; Dr Shi, J.; Silvio, D.; Liu, S.; Hong, W.; Lambert, C. J. Constructive Quantum Interference in Single-Molecule Benzodichalcogenophene Junctions. *Chem. - Eur. J.* **2020**, *26*, 5264–5269.

(33) Manrique, D. Z.; Huang, C.; Baghernejad, M.; Zhao, X.; Al-Owaedi, O. A.; Sadeghi, H.; Kalignedi, V.; Hong, W.; Gulcur, M.; Wandlowski, T.; Bryce, M. R.; Lambert, C. J. A quantum circuit rule for interference effects in single-molecule electrical junctions. *Nat. Commun.* **2015**, *6*, 6389.

(34) Arroyo, C. R.; Tarkuc, S.; Frisenda, R.; Seldenthuis, J. S.; Woerde, C. H. M.; Eelkema, R.; Grozema, F. C.; van der Zant, H. S. Signatures of quantum interference effects on charge transport through a single benzene ring. *J. Angew. Chem. Int. Ed.* **2013**, *52*, 3152–3155.

(35) Zotti, L. A.; Leary, E. Taming quantum interference in single molecule junctions: induction and resonance are key. *Phys. Chem. Chem. Phys.* **2020**, *22*, 5638–5646.

(36) O'Driscoll, L. J.; Bryce, M. R. Extended curly arrow rules to rationalise and predict structural effects on quantum interference in molecular junctions. *Nanoscale* **2021**, *13*, 1103–1123.

(37) Schmidt, M.; Wassy, D.; Hermann, M.; Teresa, M. G.; Agrait, N.; Zotti, L. A.; Esser, B.; Leary, E. Single-molecule conductance of dibenzopentalenes: antiaromaticity and quantum interference. *Chem. Commun.* **2021**, *57*, 745–748.

(38) Aggarwal, A.; Kalignedi, V.; Maiti, P. K. Quantum Circuit Rules for Molecular Electronic Systems: Where Are We Headed Based on the Current Understanding of Quantum Interference, Thermoelectric, and Molecular Spintronics Phenomena? *Nano Lett.* **2021**, *21*, 8532–8544.

(39) Al-Utayjawei, R. M.; Al-Owaedi, O. A. Enhancement of Thermoelectric Properties of Porphyrin-based Molecular Junctions by Fano Resonances. *J. Phys. Conf. Ser.* **2021**, *1818*, No. 012208.

(40) Obayes, M. A. I.; Al-Robayi, E. M.; Al-Owaedi, O. A. Investigation Quantum Electronic Transition of Organometallic Molecules. *J. Phys. Conf. Ser.* **2021**, *1973*, No. 012147.

(41) Gunasekaran, S.; Greenwald, J. E.; Venkataraman, L. Visualizing Quantum Interference in Molecular Junctions. *Nano Lett.* **2020**, *20*, 2843–2848.

(42) Camarasa-Gómez, M.; Hernangómez-Pérez, D.; Inkpen, M. S.; Lovat, G.; Fung, E.; Roy, X.; Venkataraman, L.; Evers, F. Mechanically Tunable Quantum Interference in Ferrocene-Based Single-Molecule Junctions. *Nano Lett.* **2020**, *20*, 6381–6386.

(43) Lambert, C. J. Basic concepts of quantum interference and electron transport in single-molecule electronics. *Chem. Soc. Rev.* **2015**, *44*, 875–888.

(44) Chen, H.; Golder, M. R.; Wang, F.; Jasti, R.; Swan, A. K. Raman spectroscopy of carbon nanohoops. *Carbon* **2014**, *67*, 203–213.

(45) Patel, V. K.; Kayahara, E.; Yamago, S. Practical Synthesis of [n] Cycloparaphenylenes (n = 5, 7–12) by H<sub>2</sub>SnCl<sub>4</sub>-Mediated Aromatization of 1,4-Dihydroxycyclo-2,5-diene Precursors. *Chem. - Eur. J.* **2015**, *21*, 5742–5749.

(46) Leonhardt, E. J.; Jasti, R. Emerging applications of carbon nanohoops. *Nat. Rev. Chem.* **2019**, *3*, 672–686.

(47) Liu, Z.; Lu, T. Optical Properties of Novel Conjugated Nanohoops: Revealing the Effects of Topology and Size. *J. Phys. Chem. C* **2020**, *124*, 7353–7360.

(48) Huang, X.; Bai, X.; Gan, P.; Liu, W.; Yan, H.; Gao, F.; Xu, H.; Su, Z. Design of D- $\pi$ -A type carbon nanohoops with enhanced nonlinear optical response: a size-dependent effect study. *New J. Chem.* **2023**, *47*, 5390–5398.

(49) Li, N.; Sun, M. Optical Physical Mechanisms of Helicene Carbon Nanohoop with Möbius Topology. *ChemPhysChem* **2023**, *24*, No. e202200846.

(50) Perdew, J. P.; Burke, K.; Ernzerhof, M. Generalized Gradient Approximation Made Simple. *Phys. Rev. Lett.* **1996**, *77*, 3865.

(51) Stephens, P. J.; Devlin, F. J.; Chabalowski, C. F.; Frisch, M. J. Ab Initio Calculation of Vibrational Absorption and Circular Dichroism Spectra Using Density Functional Force Fields. *J. Phys. Chem. A* **1994**, *98*, 11623–11627.

(52) Perdew, J. P.; Wang, Y. Accurate and simple analytic representation of the electron-gas correlation energy. *Phys. Rev. B* **1992**, *45*, 13244.

(53) Ferrer, J.; Lambert, C. J.; García-Suárez, V. M.; Zs Manrique, D.; Visontai, D.; Oroszlany, L.; Rodríguez-Ferradás, R.; Grace, I.; S Bailey, W. D.; Gillemot, K.; Sadeghi, H.; Algharagholy, L. A. GOLLUM: a next-generation simulation tool for electron, thermal and spin transport. *New J. Phys.* **2014**, *16*, No. 093029.

(54) Jirásek, M.; Anderson, H. L.; Peeks, M. D. From Macrocycles to Quantum Rings: Does Aromaticity Have a Size Limit? *Acc. Chem. Res.* **2021**, *54*, 3241–3251.

(55) Judd, C. J.; Nizovtsev, A. S.; Plougmann, R.; Kondratuk, D. V.; Anderson, H. L.; Besley, E.; Saywell, A. Molecular Quantum Rings Formed from a  $\pi$ -Conjugated Macrocyclic. *Phys. Rev. Lett.* **2020**, *125*, No. 206803.

(56) Chen, Z.; Deng, J.; Hou, S.; Bian, X.; Swett, J. L.; Wu, Q.; Baugh, J.; Bogani, L.; Briggs, G. A. D.; Mol, J. A.; Lambert, C. J.; Anderson, H. L.; Thomas, J. O. Phase-Coherent Charge Transport through a Porphyrin Nanoribbon. *J. Am. Chem. Soc.* **2023**, *145*, 15265–15274.

(57) Richert, S.; Cremers, J.; Kuprov, I.; Peeks, M. D.; Anderson, H. L.; Timmel, C. R. Constructive quantum interference in a bis-copper six-porphyrin nanoring. *Nat. Commun.* **2017**, *8*, No. 14842.

(58) Limburg, B.; Thomas, J. O.; Holloway, G.; Sadeghi, H.; Sangtarash, S.; Cremers, J.; Narita, A.; Müllen, K.; Lambert, C. J.; Andrew, G. D.; Mol, B. J.; Anderson, H. L. Anchor Groups for Graphene-Porphyrin Single-Molecule Transistors. *Adv. Funct. Mater.* **2018**, *28*, No. 1803629.

(59) Sedghi, G.; Esdaile, L. J.; Anderson, H. L.; García-Suárez, V. M.; Lambert, C. J.; Martin, S.; Bethell, D.; Higgins, S. J.; Nichols, R. J. Long-range electron tunnelling in oligo-porphyrin molecular wires. *Nat. Nanotechnol.* **2011**, *6*, 517–523.

(60) Algethami, N.; Sadeghi, H.; Sangtarash, S.; Lambert, C. J. The Conductance of Porphyrin-Based Molecular Nanowires Increases with Length. *Nano Lett.* **2018**, *18*, 4482–4486.

(61) Leary, E.; Limburg, B.; Sangtarash, S.; Alanazy, A.; Grace, I.; Swada, K.; Esdaile, L. J.; Noori, M. M.; González, T.; Rubio-Bollinger, G.; Sadeghi, H.; Agrait, N.; Hodgson, A.; Higgins, S. J.; Lambert, C. J.; Anderson, H. L.; Nichols, R. Bias-Driven Conductance Increase with Length in Porphyrin Tapes. *J. Am. Chem. Soc.* **2018**, *140*, 12877–12883.

(62) Becke, A. D. Density-functional thermochemistry. III. The role of exact exchange. *J. Chem. Phys.* **1993**, *98*, 5648–5652.

(63) Petersson, G. A.; Bennett, A.; Tensfeldt, T. G.; Al-Laham, M. A.; Shirley, W. A.; Mantzaris, J. A complete basis set model chemistry. I. The total energies of closed-shell atoms and hydrides of the first-row elements. *J. Chem. Phys.* **1988**, *89*, 2193–2198.

(64) Petersson, G. A.; Al-Laham, M. A. A complete basis set model chemistry. II. Open-shell systems and the total energies of the first-row atoms. *J. Chem. Phys.* **1991**, *94*, 6081–6090.

(65) Erich, R.; Gross, E. K. U. Density-Functional Theory for Time-Dependent Systems. *Phys. Rev. Lett.* **1984**, *52*, 997–1000.

(66) Scott, L. T.; Boorum, M. M.; McMahon, B. J.; Hagen, S.; Mack, J.; Blank, J.; Wegner, H.; de Meijere, A. A Rational Chemical Synthesis of C<sub>60</sub>. *Science* **2002**, *295*, 1500–1503.

- (67) Lambert, C. J. *Quantum Transport in Nanostructures and Molecules: An Introduction to Molecular Electronics*; IOP, 2021; p 15.
- (68) Lambert, C. J.; Liu, S.-X. A Magic Ratio Rule for Beginners: A Chemist's Guide to Quantum Interference in Molecules. *Chem. - Eur. J.* **2018**, *24*, 4193–4201.
- (69) Coulson, C. A.; Rushbrooke, G. S. Note on the method of molecular orbitals. *Math. Proc. Cambridge Philos. Soc.* **1940**, *36*, 193–200.
- (70) Yoshizawa, K. An Orbital Rule for Electron Transport in Molecules. *Acc. Chem. Res.* **2012**, *45*, 1612–1621.
- (71) Tada, T.; Yoshizawa, K. Molecular design of electron transport with orbital rule: toward conductance-decay free molecular junctions. *Phys. Chem. Chem. Phys.* **2015**, *17*, 32099–32110.
- (72) Tsuji, Y.; Yoshizawa, K. Frontier Orbital Perspective for Quantum Interference in Alternant and Nonalternant Hydrocarbons. *J. Phys. Chem. C* **2017**, *121*, 9621–9626.
- (73) Okazawa, K.; Tsuji, Y. Y.; Yoshizawa, K. Understanding Single-Molecule Parallel Circuits on the Basis of Frontier Orbital Theory. *J. Phys. Chem. C* **2020**, *124*, 3322–3331.
- (74) Camarasa-Gómez, M.; Hernangómez-Pérez, D.; Inkpen, M. S. G.; Lovat, E.; Fung, E.; Roy, X.; Venkataraman, L.; Evers, F. Mechanically Tunable Quantum Interference in Ferrocene-Based Single-Molecule Junctions. *Nano Lett.* **2020**, *20*, 6381–6386.
- (75) Al-Owaedi, O. A. Thermoelectric Properties of Porphyrin Nano Rings: A Theoretical and Modelling Investigation. *ChemPhysChem* **2023**, No. e202300616.
- (76) Graham, A. R.; Dan, H. M.; Robin, J. N.; Andrei, N. K. UV–vis absorption spectroscopy of carbon nanotubes: Relationship between the p-electron plasmon and nanotube diameter. *Chem. Phys. Lett.* **2010**, *493*, 19–23.
- (77) Nijegorodov, N. I.; Downey, W. S.; Danailov, M. B. Systematic investigation of absorption, fluorescence and laser properties of some p- and m-oligophenylenes. *Spectrochim. Acta, Part A* **2000**, *56*, 783–795.
- (78) Yang, G.; Li, J.; Deng, X.; Song, X.; Lu, M.; Zhu, Y.; Yu, Z.; Xu, B.; Li, M.; Dang, L. Construction and Application of Large Stokes-Shift Organic Room Temperature Phosphorescence Materials by Intermolecular Charge Transfer. *J. Phys. Chem. Lett.* **2023**, *14*, 6927–6934.
- (79) Lohani, A.; Durgapal, S.; Morganti, P. *Quantum Dots: An Emerging Implication of Nanotechnology in Cancer Diagnosis and Therapy*; Elsevier, 2023; pp 243–262.
- (80) Qi, O.; Qian, P.; Zhigang, S. Computational screen-out strategy for electrically pumped organic laser materials. *Nat. Commun.* **2020**, *11*, No. 4485.
- (81) Deshpande, A. V.; Beidoun, A.; Penzkofer, A.; Wagenblast, G. Absorption and emission spectroscopic investigation of cyanovinylidethylaniline dye vapors. *Chem. Phys.* **1990**, *142*, 123–131.
- (82) Büttiker, M.; Landauer, R. Traversal Time for Tunneling. *Phys. Rev. Lett.* **1982**, *49*, 1739–1742.
- (83) Xiang, D.; Wang, X.; Jia, C.; Lee, T.; Guo, X. Molecular-Scale Electronics: From Concept to Function. *Chem. Rev.* **2016**, *116*, 4318–4440.
- (84) Salman, S. R.; Al-Owaedi, O. A. Theoretical Investigation and Prediction of Promising Organic Molecules for Optical and Electronic Applications. *HIV Nursing* **2023**, *23*, 321–326.
- (85) Chen, R.; Sharony, I.; Nitzan, A. Local Atomic Heat Currents and Classical Interference in Single-Molecule Heat Conduction. *J. Phys. Chem. Lett.* **2020**, *11*, 4261–4268.
- (86) Wu, C.; Bates, D.; Sangtarash, S.; Ferri, N.; Thomas, A.; Higgins, S. J.; Robertson, C. M.; Nichols, R. J.; Sadeghi, H.; Vezzoli, A. Folding a Single-Molecule Junction. *Nano Lett.* **2020**, *20*, 7980–7986.
- (87) Miao, R.; Xu, H.; Skripnik, M.; Cui, L.; Wang, K.; Pedersen, K. G. L.; Leijnse, M.; Pauly, F.; Wärmarm, K.; Meyhofer, E.; Reddy, P.; Linke, H. Influence of Quantum Interference on the Thermoelectric Properties of Molecular Junctions. *Nano Lett.* **2018**, *18*, 5666–5672.
- (88) Stefani, D.; Weiland, K. J.; Skripnik, M.; Hsu, C.; Perrin, M. L.; Mayor, M.; Pauly, F.; van der Zant, H. S. J. Large Conductance Variations in a Mechanosensitive Single-Molecule Junction. *Nano Lett.* **2018**, *18*, 5981–5988.
- (89) Jones, L. O.; Mosquera, M. A.; Fu, B.; Schatz, G. C.; Marks, T. J.; Ratner, M. A. Quantum Interference and Substantial Property Tuning in Conjugated Z-ortho-Regio-Resistive Organic (ZORRO) Junctions. *Nano Lett.* **2019**, *19*, 8956–8963.
- (90) Huang, B.; Liu, X.; Yuan, Y.; Hong, Z.; Zheng, J.; Pei, L.; Shao, Y.; Li, J.; Zhou, X.; Chen, J.; Jin, S.; Mao, B. Controlling and Observing Sharp-Valleyed Quantum Interference Effect in Single Molecular Junctions. *J. Am. Chem. Soc.* **2018**, *140*, 17685–17690.
- (91) Moreno-Garcia, P.; Gulcur, M.; Manrique, D. Z.; Pope, T.; Hong, W. J.; Kaliginedi, V.; Huang, C. C.; Batsanov, A. S.; Bryce, M. R.; Lambert, C. J.; Wandlowski, T. Single-Molecule Conductance of Functionalized Oligoynes: Length Dependence and Junction Evolution. *J. Am. Chem. Soc.* **2013**, *135*, 12228–12240.
- (92) Kim, B.; Beebe, J. M.; Olivier, C.; Rigaut, S.; Touchard, D.; Kushmerick, J. G.; Zhu, X. Y.; Frisbie, C. D. Temperature and length dependence of charge transport in redox-active molecular wires incorporating ruthenium(II) bis(F-arylacetylide) complexes. *J. Phys. Chem. C* **2007**, *111*, 7521–7526.
- (93) Lu, Q.; Liu, K.; Zhang, H. M.; Du, Z. B.; Wang, X. H.; Wang, F. S. From Tunneling to Hopping: A Comprehensive Investigation of Charge Transport Mechanism in Molecular Junctions Based on Oligo(p-phenylene ethynylene)s. *ACS Nano* **2009**, *3*, 3861–3868.
- (94) Garner, M. H.; Li, H. X.; Chen, Y.; Su, T. A.; Shanggun, Z.; Paley, D. W.; Liu, T. F.; Ng, F.; Li, H. X.; Xiao, S. X.; Nuckolls, C.; Venkataraman, L.; Solomon, G. C. Comprehensive suppression of single-molecule conductance using destructive sigma-interference. *Nature* **2018**, *558*, 415–419.
- (95) Burkle, M.; Hellmuth, T. J.; Pauly, F.; Asai, Y. First-principles calculation of the thermoelectric figure of merit for [2,2]-paracyclophane-based single-molecule junctions. *Phys. Rev. B* **2015**, *91*, No. 165419.
- (96) Putatunda, A.; Singh, D. J. Lorenz number in relation to estimates based on the Seebeck coefficient. *Mater. Today Phys.* **2019**, *8*, 49–55.
- (97) Hung, N. T.; Nugraha, A. R. T.; Saito, R. Thermoelectric Properties of Carbon Nanotubes. *Energies* **2019**, *12*, 4561.
- (98) Al-Mammory, B. A. A.; Al-Owaedi, O. A.; Al-Robayi, E. M. Thermoelectric Properties of Oligoynes-Molecular Wires. *J. Phys. Conf. Ser.* **2021**, *1818*, No. 012095.
- (99) Shelykh, I. A.; Bagraev, N. T.; Klyachkin, L. E. Spin depolarization in spontaneously polarized low-dimensional systems. *Semiconductors* **2003**, *37*, 1390–1399.
- (100) Chen, J.; Reed, M. A.; Rawlett, A. M.; Tour, J. M. Large On-Off Ratios and Negative Differential Resistance in a Molecular Electronic Device. *Science* **1999**, *286*, 1550–1552.
- (101) Reed, M. A.; Zhou, C.; Muller, C. J.; Burgin, T. P.; Tour, J. M. Conductance of a Molecular Junction. *Science* **1997**, *278*, 252–254.
- (102) Xu, B. Q.; Tao, N. J. Measurement of Single-Molecule Resistance by Repeated Formation of Molecular Junctions. *Science* **2003**, *301*, 1221–1223.
- (103) Jia, C.; Guo, X. Molecule–electrode interfaces in molecular electronic devices. *Chem. Soc. Rev.* **2013**, *42*, 5642–5660.
- (104) Venkataraman, L.; Klare, J. E.; Nuckolls, C.; Hybertsen, M. S.; Steigerwald, M. L. Dependence of single-molecule junction conductance on molecular conformation. *Nature* **2006**, *442*, 904–907.
- (105) Manrique, D. Z.; Huang, C.; Baghernejad, M.; Zhao, X.; Al-Owaedi, O. A.; Sadeghi, H.; Kaliginedi, V.; Hong, W.; Gulcur, M.; Wandlowski, T.; Bryce, M. R.; Lambert, C. J. A quantum circuit rule for interference effects in single-molecule electrical junctions. *Nat. Commun.* **2015**, *6*, 6389.
- (106) Al-Owaedi, O. A.; Milan, D. C.; Oerthel, M.; Bock, S.; Yufit, D. S.; Howard, J. A. K.; Higgins, S. J.; Nichols, R. J.; Lambert, C. J.; Bryce, M. R.; Low, P. J. Experimental and Computational Studies of the Single-Molecule Conductance of Ru(II) and Pt(II) trans-Bis(acetylide) Complexes. *Organometallics* **2016**, *35*, 2944–2954.
- (107) Ballmann, S.; Härtle, R.; Coto, P. B.; Elbing, M.; Mayor, M.; Bryce, M. R.; Thoss, M.; Weber, H. B. Experimental Evidence for Quantum Interference and Vibrationally Induced Decoherence in Single-Molecule Junctions. *Phys. Rev. Lett.* **2012**, *109*, No. 056801.

- (108) Eichler, J. C. A.; Ceballos, J. M. G.; Rurali, R.; Bachtold, A. A nanomechanical mass sensor with yoctogram resolution. *Nano-technol.* **2012**, *7*, 301–304.
- (109) Finch, C. M.; Garcia-Suarez, V. M.; Lambert, C. J. Giant thermopower and figure of merit in single-molecule devices. *Phys. Rev. B* **2009**, *79*, No. 033405.
- (110) Al-Owaedi, O. A.; Khalil, T. T.; Karim, S. A.; Said, M. H.; Al-Bermany, E.; Taha, D. N. The promising barrier: Theoretical investigation. *Syst. Rev. Pharm.* **2020**, *11*, 110–115.
- (111) Ozawa, H.; Baghernejad, M.; Al-Owaedi, O. A.; Kaliginedi, V.; Nagashima, T.; Ferrer, J.; Wandlowski, T.; García-Suárez, V. M.; Broekmann, P.; Lambert, C. J.; Haga, M. Synthesis and Single-Molecule Conductance Study of Redox-Active Ruthenium Complexes with Pyridyl and Dihydrobenzo[b]thiophene Anchoring Groups. *Chem.-Eur. J.* **2016**, *22*, 12732–12740.
- (112) Sivan, U.; Imry, Y. Multichannel Landauer formula for thermoelectric transport with application to thermopower near the mobility edge. *Phys. Rev. B* **1986**, *33*, 551.
- (113) Hanwell, M. D.; Curtis, D. E.; Lonie, D. C.; Vandermeersch, T.; Zurek, E.; Hutchison, G. R. Avogadro: an advanced semantic chemical editor, visualization, and analysis platform. *J. Cheminf.* **2012**, *4*, 1–17.
- (114) Schlegel, H. B. J.; Binkley, S.; Pople, J. A. First and second derivatives of two electron integrals over Cartesian Gaussians using Rys polynomials. *J. Chem. Phys.* **1984**, *80*, 1976–1981.
- (115) Naher, M.; Milan, D. C.; Al-Owaedi, O. A.; Planje, I. J.; Bock, S.; Hurtado-Gallego, J.; Bastante, P.; Dawood, Z. M. A.; Rincón-García, L.; Rubio-Bollinger, G.; Higgins, S. J.; Agraït, N.; Lambert, C. J.; Nichols, R. J.; Low, P. J. Molecular structure–(thermo) electric property relationships in single-molecule junctions and comparisons with single- and multiple-parameter models. *J. Am. Chem. Soc.* **2021**, *143* (10), 3817–3829.